J. Fluid Mech. (1968), *vol.* 34, *part* 1, *pp.* 177–205
Printed in Great Britain

The stability of steady and time-dependent plane Poiseuille flow

By CHESTER E. GROSCH

Hudson Laboratories of Columbia University,
Dobbs Ferry, New York 10522

AND HAROLD SALWEN

Stevens Institute of Technology, Hoboken, New Jersey, 07030 and
Hudson Laboratories of Columbia University, Dobbs Ferry,
New York 10522

(Received 24 November 1967 and in revised form 22 April 1968)

The linear stability of plane Poiseuille flow has been studied both for the steady flow and also for the case of a pressure gradient that is periodic in time. The disturbance streamfunction is expanded in a complete set of functions that satisfy the boundary conditions. The expansion is truncated after N terms, yielding a set of N linear first-order differential equations for the time dependence of the expansion coefficients.

For the steady flow, calculations have been carried out for both symmetric and antisymmetric disturbances over a wide range of Reynolds numbers and disturbance wave-numbers. The neutral stability curve, curves of constant amplification and decay rate, and the eigenfunctions for a number of cases have been calculated. The eigenvalue spectrum has also been examined in some detail. The first N eigenvalues are obtained from the numerical calculations, and an asymptotic formula for the higher eigenvalues has been derived. For those values of the wave-number and Reynolds number for which calculations were carried out by L. H. Thomas, there is excellent agreement in both the eigenvalues and the eigenfunctions with the results of Thomas.

For the time-dependent flow, it was found, for small amplitudes of oscillation, that the modulation tended to stabilize the flow. If the flow was not completely stabilized then the growth rate of the disturbance was decreased. For a particular wave-number and Reynolds number there is an optimum amplitude and frequency of oscillation for which the degree of stabilization is a maximum. For a fixed amplitude and frequency of oscillation the wave-number of the disturbance and the Reynolds number has been varied and a neutral stability curve has been calculated. The neutral stability curve for the modulated flow shows a higher critical Reynolds number and a narrower band of unstable wave-numbers than that of the steady flow. The physical mechanism responsible for this stabilization appears to be an interference between the shear wave generated by the modulation and the disturbance.

For large amplitudes, the modulation destabilizes the flow. Growth rates of

the modulated flow as much as an order of magnitude greater than that of the steady unmodulated flow have been found.

1. Introduction

There is a considerable body of theoretical literature on the solution of the Orr–Sommerfeld equation for steady plane Poiseuille flow. The application of asymptotic methods of analysis to this problem has been summarized by Lin (1955), Stuart (1963), Shen (1964) and Reid (1965). Thomas (1953) has used numerical methods to obtain the eigenvalues with high accuracy for a number of values of the disturbance wave-number and flow Reynolds number. All of these solutions, however, are for the least stable eigenmode only, and most of them are restricted to values of the wave-number and Reynolds number which are close to the stability boundary.

To our knowledge, only Southwell & Chitty (1930), Grohne (1954) and Gallagher & Mercer (1964) have reported calculations of any of the higher eigenvalues for any plane parallel flow. Southwell & Chitty, Grohne and Gallagher & Mercer reported the first four eigenvalues for plane Couette flow. There is satisfactory agreement between the results of Southwell & Chitty and those of Gallagher & Mercer. There are, however, considerable differences between Grohne's results and those of the others. Grohne has also calculated the first four eigenvalues for plane Poiseuille flow.

In contrast to the above situation, very little theoretical work has been done on the stability of time-dependent flows (see, however, Shen 1961; Greenspan & Benney 1963; Kelly 1965, 1967; Conrad & Criminale 1965*a*, *b*), though two recent experimental studies of the stability of periodically modulated flows make a better understanding of this subject highly desirable.

These experiments are studies of modulated Couette flow (Donnelly, Reif & Suhl 1962; Donnelly 1964) and modulated Poiseuille flow (Gilbrech & Combs 1963). In the Couette flow experiment, the outer cylinder was stationary and the inner cylinder was rotated. The rotational speed of the inner cylinder was sinusoidally modulated, and the amplitude of modulation, as well as the modulation frequency, was varied. It was found that in all cases the onset of instability was inhibited by modulating the rotational speed of the inner cylinder. The degree of inhibition was dependent on the modulation amplitude and frequency. At the optimum frequency the flow was stable, provided that the angular velocity dropped below the critical angular velocity at some point in the cycle. In the Poiseuille flow experiment the pressure gradient in the pipe was sinusoidally modulated, disturbances were generated in the flow, and the growth rate was measured. The experimental results indicated that, if the modulation frequency is held fixed and the amplitude of the pressure modulation is increased from zero, the critical Reynolds number first increases and then decreases. The increase in the critical Reynolds number can be quite large; at one modulation frequency the critical Reynolds number was more than doubled. The amplitude at which the critical Reynolds number is a maximum appears to decrease with increasing frequency of modulation.

There is further interest in the stability of time-dependent flows since it appears that the laminar–turbulent transition of a steady flow is connected to the instability of a time-dependent shear flow. It has been suggested (Greenspan & Benney 1963) that, in order to understand the later stages of the laminar–turbulent transition, the linear stability of the time-dependent flow formed by the superposition of the primary instabilities and steady base flow should be studied.

In the work reported in this paper, we have studied the stability of plane Poiseuille flow by the method of expansion in a set of orthogonal functions. This is the method used in the first successful theoretical study of hydrodynamic stability—Taylor's (1923) solution of the Couette flow problem—but it has been given little use in recent years. The three recent applications of this method of which we are aware are studies of generalized Couette flows by Chandrasekhar and co-workers (Chandrasekhar 1961), of plane Couette flows by Gallagher & Mercer (1962, 1964), and of plane Poiseuille flow by Dolph & Lewis (1958). We will comment briefly on the latter study, since it deals (as does ours) with plane Poiseuille flow.

Dolph & Lewis used an expansion technique to study the stability of steady plane Poiseuille flow. They calculated a neutral stability curve using an eight-term expansion and also obtained a few results with a twenty-term approximation. The results obtained with the eight-term approximation are in very poor agreement with the results of both the asymptotic theory and Thomas's (1953) numerical calculations. However, the scattered results obtained with the twenty-term approximation show better agreement. The improved results with a twenty-term expansion suggest that with more terms Dolph & Lewis might have obtained high accuracy; but the poor agreement obtained with the eight-term approximation apparently convinced many workers in this field of the unsuitability of expansion techniques in the study of hydrodynamic stability. (See, for example, Reid 1965.)

In § 2 of this paper we apply the method of expansion in orthogonal functions to the problem of the linear stability of time-dependent, plane Poiseuille flow. The results for steady flow are presented in § 3 and the results for the modulated flow are given in § 4. Section 5 contains a summary of the results and a discussion of their significance.

A few of the results reported in this paper have been previously reported in abbreviated form (Grosch & Salwen 1967).

2. Analysis

2.1. *Formulation*

We wish to study the linear stability of time-dependent plane Poiseuille flow of an incompressible fluid. The distance between the plates that form the upper and lower boundaries is l. The pressure distributions which we consider here will always have a steady component so that the flow will always have a steady component with a parabolic profile. The maximum speed of this parabolic profile we denote by U_0.

Throughout the remainder of this paper dimensionless variables will be used. The co-ordinates are measured in units of l and velocities in units of U_0. The time scale is (l/U_0) and the pressure scale is ρU_0^2, where ρ is the density. In terms of the dimensionless variables the boundaries are at $y = \pm\frac{1}{2}$. The velocity distribution of the base flow in terms of the dimensionless variables will be written as $U(y,t)$. The Reynolds number of the flow is $R = U_0 l/\nu$, where $\nu = \mu/\rho$ is the kinematic viscosity of the fluid, and is exactly twice the Reynolds number as defined by Lin and Thomas.

It is assumed that the streamfunction of a small perturbation to the base flow can be written in the form

$$\psi(x,y,t) = \phi(y,t)\, e^{i\alpha x}, \tag{1}$$

where α is the dimensionless wave-number of the disturbance. (The wave-number in these units is exactly twice that of Lin and Thomas.) After linearizing the Navier–Stokes equations and eliminating the pressure, it is found that $\phi(y,t)$, the amplitude of the disturbance streamfunction, must satisfy

$$L\left(\frac{\partial\phi}{\partial t}\right) = \left\{R^{-1}L^2 + i\alpha\left[\frac{\partial^2 U}{\partial y^2} - UL\right]\right\}\phi \equiv \mathscr{L}\phi, \tag{2}$$

where $L \equiv (\partial^2/\partial y^2) - \alpha^2$ and R is the Reynolds number. This is just the time-dependent version of the Orr–Sommerfeld equation. The boundary condition is that the disturbance velocity vanishes on the boundaries and hence that

$$\phi = \frac{\partial\phi}{\partial y} = 0 \quad \text{at} \quad y = \pm\tfrac{1}{2}. \tag{3}$$

The approach to be followed is to expand $\phi(y,t)$ in a complete set of functions of y which satisfy the boundary conditions. The expansion coefficients are functions of time and from equation (2) a set of differential equations governing the time dependence of these expansion coefficients will be derived.

2.2. *Expansion functions*

There are, of course, a number of possible choices of expansion functions. A convenient choice is the set of eigenfunctions of L^2 which satisfy the boundary conditions (3). That is, the expansion functions are the solutions of

$$L^2 G = \lambda^4 G \tag{4}$$

or

$$G^{\mathrm{iv}} - 2\alpha^2 G'' + (\alpha^4 - \lambda^4)G = 0 \tag{5}$$

with

$$G(\pm\tfrac{1}{2}) = G'(\pm\tfrac{1}{2}) = 0. \tag{6}$$

Because of the symmetry of equations (5) and (6), the eigenfunctions are either even or odd functions of y. The eigenvalues corresponding to even eigenfunctions are denoted by λ_n and must satisfy the equation

$$\beta_n \tanh(\tfrac{1}{2}\beta_n) + \gamma_n \tan(\tfrac{1}{2}\gamma_n) = 0, \tag{7}$$

where

$$\beta_n = (\lambda_n^2 + \alpha^2)^{\frac{1}{2}}, \quad \gamma_n = (\lambda_n^2 - \alpha^2)^{\frac{1}{2}}. \tag{8}$$

The corresponding eigenfunctions are given by

$$C_n(y) = \bar{c}_n\left[\frac{\cosh(\beta_n y)}{\cosh(\frac{1}{2}\beta_n)} - \frac{\cos(\gamma_n y)}{\cos(\frac{1}{2}\gamma_n)}\right] \tag{9}$$

where $\bar{c}_n$ is a normalizing constant, chosen so that†

$$\langle C_n, C_m\rangle = \delta_{nm}. \tag{10}$$

The roots of equation (7) are all real and

$$\lambda_n \approx (2n-\tfrac{1}{2})\pi \tag{11}$$

except when (α/n) is large.

The eigenvalues corresponding to the odd eigenfunctions are denoted by μ_n and must satisfy the equation

$$\xi_n \coth(\tfrac{1}{2}\xi_n) - \eta_n \cot(\tfrac{1}{2}\eta_n) = 0, \tag{12}$$

where

$$\xi_n = (\mu_n^2+\alpha^2)^{\frac{1}{2}}, \quad \eta_n = (\mu_n^2-\alpha^2)^{\frac{1}{2}}. \tag{13}$$

The corresponding eigenfunctions are

$$S_n(y) = \bar{s}_n\left[\frac{\sinh(\xi_n y)}{\sinh(\frac{1}{2}\xi_n)} - \frac{\sin(\eta_n y)}{\sin(\frac{1}{2}\eta_n)}\right] \tag{14}$$

and $\bar{s}_n$ is the normalizing constant. The roots of (12) are all real and

$$\mu_n \approx (2n+\tfrac{1}{2})\pi \tag{15}$$

except when (α/n) is large.

2.3. *Matrix equations*

It is assumed that ϕ can be expanded in a series in terms of the orthonormal expansion functions

$$\phi(y,t) = \sum_{n=1}^{\infty}\{a_n(t)C_n(y) + b_n(t)S_n(y)\} \tag{16}$$

so that

$$a_n(t) = \langle C_n, \phi\rangle; \quad b_n(t) = \langle S_n, \phi\rangle. \tag{17}$$

Now take the inner product of one of the functions, say $C_r(y)$, with (2):

$$\left\langle C_r, L\left(\frac{\partial\phi}{\partial t}\right)\right\rangle = \langle C_r, \mathscr{L}\phi\rangle. \tag{18}$$

After integrating by parts, the left-hand side of (18) is

$$\left\langle C_r, L\left(\frac{\partial\phi}{\partial t}\right)\right\rangle = \left\langle LC_r, \frac{\partial\phi}{\partial t}\right\rangle = \sum_{n=1}^{\infty}\langle LC_r, C_n\rangle\frac{da_n}{dt}. \tag{19}$$

The right-hand side of (18) is, after integrating by parts and using the boundary conditions,

$$\begin{aligned}\langle C_r, \mathscr{L}\phi\rangle &= R^{-1}\langle L^2C_r, \phi\rangle + i\alpha\left\langle\left(\frac{\partial^2 U}{\partial y^2} - LU\right)C_r, \phi\right\rangle \\ &= \sum_{n=1}^{\infty}\{[R^{-1}D_{rn}^{(1)} + i\alpha F_{rn}^{(1)}]a_n + i\alpha G_{rn}^{(2)}b_n\},\end{aligned} \tag{20}$$

† $\langle f, g\rangle \equiv \int_{-\frac{1}{2}}^{\frac{1}{2}} f(y)g(y)\,dy.$

where
$$D^{(1)}_{rn} = \langle L^2 C_r, C_n \rangle = \lambda_r^4 \delta_{rn}, \tag{21}$$

$$F^{(1)}_{rn} = \left\langle \frac{\partial^2 U}{\partial y^2} C_r, C_n \right\rangle - \langle L(UC_r), C_n \rangle, \tag{22}$$

and
$$G^{(2)}_{rn} = \left\langle \frac{\partial^2 U}{\partial y^2} C_r, S_n \right\rangle - \langle L(UC_r), S_n \rangle. \tag{23}$$

Thus
$$\sum_{n=1}^{\infty} \langle LC_r, C_n \rangle \frac{da_n}{dt} = \sum_{n=1}^{\infty} \{[R^{-1} D^{(1)}_{rn} + i\alpha F^{(1)}_{rn}] a_n + i\alpha G^{(2)}_{rn} b_n\}. \tag{24}$$

In an exactly similar way, taking the inner product of S_r with equation (2), it is easy to derive

$$\sum_{n=1}^{\infty} \langle LS_r, S_n \rangle \frac{db_n}{dt} = \sum_{n=1}^{\infty} \{i\alpha F^{(2)}_{rn} a_n + [R^{-1} D^{(2)}_{rn} + i\alpha G^{(1)}_{rn}] b_n\}, \tag{25}$$

with
$$D^{(2)}_{rn} = \langle L^2 S_r, S_n \rangle = \mu_r^4 \delta_{rn}, \tag{26}$$

$$G^{(1)}_{rn} = \left\langle \frac{\partial^2 U}{\partial y^2} S_r, S_n \right\rangle - \langle L(US_r), S_n \rangle, \tag{27}$$

and
$$F^{(2)}_{rn} = \left\langle \frac{\partial^2 U}{\partial y^2} S_r, C_n \right\rangle - \langle L(US_r), C_n \rangle. \tag{28}$$

Equations (24) and (25) for $r = 1, 2, 3, \ldots$ constitute the stability problem.

We now assume that the expansion for ϕ can be truncated after N terms. This truncation enables us to reduce the stability problem to a set of $2N$ linear first-order differential equations, (24) and (25), for the time dependence of the expansion coefficients. We can then rewrite equations (24) and (25) in matrix form as

$$\hat{C} \frac{d\mathbf{A}}{dt} = [R^{-1} D^{(1)} + i\alpha F^{(1)}] \mathbf{A} + i\alpha G^{(2)} \mathbf{B}, \tag{29}$$

$$\hat{S} \frac{d\mathbf{B}}{dt} = i\alpha F^{(2)} \mathbf{A} + [R^{-1} D^{(2)} + i\alpha G^{(1)}] \mathbf{B}, \tag{30}$$

where $\mathbf{A}$ and $\mathbf{B}$ are the column vectors of the $\{a_n\}$ and $\{b_n\}$,

$$[\hat{C}]_{rn} = \langle LC_r, C_n \rangle, \tag{31}$$

$$[\hat{S}]_{rn} = \langle LS_r, S_n \rangle \tag{32}$$

and $D^{(1)}$, $D^{(2)}$, $F^{(1)}$, $F^{(2)}$, $G^{(1)}$ and $G^{(2)}$ are the $(N \times N)$ matrices whose elements are $D^{(1)}_{rn}$, $D^{(2)}_{rn}$, etc. After multiplying by $\hat{C}^{-1}$ and $\hat{S}^{-1}$ we have

$$\frac{d}{dt} \begin{pmatrix} \mathbf{A} \\ \mathbf{B} \end{pmatrix} = \begin{pmatrix} F & J \\ K & G \end{pmatrix} \begin{pmatrix} \mathbf{A} \\ \mathbf{B} \end{pmatrix}, \tag{33}$$

where
$$F = \hat{C}^{-1}[R^{-1} D^{(1)} + i\alpha F^{(1)}], \tag{34}$$

$$J = \hat{C}^{-1}[i\alpha G^{(2)}], \tag{35}$$

$$K = \hat{S}^{-1}[i\alpha F^{(2)}], \tag{36}$$

$$G = \hat{S}^{-1}[R^{-1} D^{(2)} + i\alpha G^{(1)}]. \tag{37}$$

2.4. *Stability criterion*

Before proceeding further we shall discuss the criterion for stability in the case of steady and periodic flows. In §2.5 we shall formulate the stability problem for our truncated matrix equation (33).

In the study of the linear stability of a steady flow it is customary (Lin 1955) to look for solutions to equations (2) and (3) with an $e^{\sigma t}$ time dependence. If, for any such solution, the real part of σ is positive, the flow is clearly unstable since the disturbance grows exponentially with the time. If, for all such solutions, the real part of σ is negative, it is concluded that the flow is stable against infinitesimal disturbances.

This conclusion is based on the assumption that equations (2) and (3) possess a complete set of solutions of the form $\psi(y)\, e^{\sigma t}$ or, equivalently, that the infinite matrix equation

$$\sigma \begin{pmatrix} \hat{C} & 0 \\ 0 & \hat{S} \end{pmatrix} \begin{pmatrix} \mathbf{A} \\ \mathbf{B} \end{pmatrix} = \begin{pmatrix} R^{-1}D^{(1)} + i\alpha F^{(1)} & i\alpha G^{(2)} \\ i\alpha F^{(2)} & R^{-1}D^{(2)} + i\alpha G^{(1)} \end{pmatrix} \begin{pmatrix} \mathbf{A} \\ \mathbf{B} \end{pmatrix} \tag{38}$$

has a complete set of eigenvectors. The proof of this conclusion is difficult because the matrices involved are not Hermitian, but it has been carried out by Schensted (1960) for the case of plane Poiseuille flow (which we are studying) and by Haupt (1912) for the case of plane Couette flow. The proofs were dependent upon the form of the base flow.

If the base flow is periodic with period τ, we expect (by analogy with Floquet's theorem) to have a complete set of solutions of the form

$$\psi(y,t)\, e^{\sigma t}, \tag{39}$$

where ψ is a periodic function of the time with period τ, so that the flow will be unstable to infinitesimal disturbances if and only if at least one σ has a positive real part. This may be justified as follows.

Let $\{\tilde{\phi}_n(y)\}$ be a complete set of functions satisfying the boundary conditions (3) and let $\{\phi_n(y,t)\}$ be the solutions to equations (2) and (3) such that

$$\phi_n(y,0) = \tilde{\phi}_n(y). \tag{40}$$

Then $\phi_n(y,\tau)$ may be expanded in $\{\tilde{\phi}_n\}$:

$$\phi_n(y,\tau) = \sum_m \langle \tilde{\phi}_m(y), \phi_n(y,\tau)\rangle \tilde{\phi}_m(y). \tag{41}$$

The coefficients $\langle \tilde{\phi}_m(y), \phi_n(y,\tau)\rangle$ define the transformation T from $t=0$ to $t=\tau$ for a general function satisfying the boundary conditions (3) for, if $f(y)$ is any such function, then

$$\phi(y,t) \equiv \sum_n \langle \tilde{\phi}_n, f\rangle \phi_n(y,t) \tag{42}$$

is a solution to (2) and (3) such that

$$\phi(y,0) = f(y) \tag{43}$$

and

$$T[f(y)] \equiv \phi(y,\tau) = \sum_{n,m} \langle \tilde{\phi}_m(y), \phi_n(y,\tau)\rangle \langle \tilde{\phi}_n, f\rangle \tilde{\phi}_m(y). \tag{44}$$

Now let $\tilde{\phi}_\epsilon(y)$ be an eigenfunction of T so

$$T\tilde{\psi}_\epsilon = \epsilon \tilde{\psi}_\epsilon, \tag{45}$$

and define
$$\psi_\epsilon(y,t) \equiv \sum_n \langle \tilde{\phi}_n, \tilde{\psi}_\epsilon \rangle \phi_n(y,t)\, e^{-\sigma t}, \tag{46}$$

where
$$\sigma = (\ln \epsilon)/\tau. \tag{47}$$

Then
$$\psi_\epsilon(y,\tau) = e^{-\sigma t} T \tilde{\psi}_\epsilon(y) = \tilde{\psi}_\epsilon(y) = \psi_\epsilon(y,0). \tag{48}$$

So
$$\psi_\epsilon(y,t)\, e^{\sigma t} \tag{49}$$

is a solution of equations (2) and (3) of the desired form. There will be a complete set of solutions of the form (39), $\psi(y,t)\, e^{\sigma t}$, with periodic ψ, if and only if T has a complete set of eigenfunctions.

It is reasonable to assume that T does possess a complete eigenvalue spectrum but, in view of the difficulties encountered in the steady case, it is likely that the proof of this fact would be extremely difficult. In any case, the solutions to the truncated problem (33) are of the form (39) since the matrices are finite.

2.5. *Stability criterion for the truncated problem*

If the coefficient matrix in (33) is periodic then (Coddington & Levenson 1955) there exists a fundamental solution matrix $W(t)$ which is a solution of

$$\frac{dW}{dt} = \begin{pmatrix} F & J \\ K & G \end{pmatrix} W, \tag{50}$$

$$W(0) = I,$$

where I is the identity matrix and W is of the form

$$W(t) = P(t) \exp(tQ), \tag{51}$$

where P is a periodic non-singular matrix whose period is the same as that of the coefficient matrix, and Q is a constant matrix. The transformation T discussed in the previous section is just $W(\tau)$.

The eigenvalues of Q can be found rather simply by integrating equation (50) from $t = 0$ to $t = \tau$, then

$$\begin{aligned} W(\tau) &= P(\tau) \exp(\tau Q) \\ &= P(0) \exp(\tau Q) \\ &= \exp(\tau Q) \end{aligned} \tag{52}$$

after noting that P is periodic. If $\{\epsilon_j\}\,(j = 1, 2, 3, \ldots, N)$ are the eigenvalues of $W(\tau)$, then $\{\sigma_j\}\,(j = 1, 2, 3, \ldots, N)$, the eigenvalues of Q, are

$$\sigma_j = \ln(\epsilon_j)/\tau. \tag{53}$$

The stability characteristics of the flow are determined by the real part of the σ_j's. It should be noted that $\mathrm{Im}(\sigma_j)$ is only defined modulo $(2\pi/\tau)$.

3. Results for steady plane Poiseuille flow

The base flow velocity profile is, for the steady flow,

$$U = 1 - 4y^2, \quad |y| \leqslant \tfrac{1}{2}. \tag{54}$$

Since U is symmetric, the cross-coupling matrices J and K are identically zero and, hence, symmetric and antisymmetric disturbances are uncoupled. It has been customary (Lin 1955) to consider only those disturbances which have a symmetric streamfunction. However, we will consider disturbances with both symmetric and antisymmetric streamfunctions. The calculation of the matrix elements of F and G, equations (34) and (37), is tedious but presents no special difficulties.

The eigenvalues of the matrices were computed numerically using the QR algorithm (Wilkinson 1965; Parlett 1967). The determination of all the eigenvalues of F, when F is 30×30, takes about one minute on an IBM 7094 and the running time is proportional to N^3. The output of the computer program is the N values of $[\sigma_j]$. In order to facilitate comparison with the results of other investigations, we will give our results for the values of the complex wave speed,

$$c_j = \sigma_j / i\alpha. \tag{55}$$

The flow will be unstable if, for some j,

$$\mathrm{Im}\,(c_j) < 0. \tag{56}$$

The eigenvalues are numbered in order of increasing imaginary part of c_j. The order is taken to be that at small R.

3.1. *Accuracy of the calculations*

There are a number of checks on the results of the calculation. A check on the performance of the eigenvalue routine is provided by a comparison of the sum of the eigenvalues with the trace. It was found in all cases that the sum of the eigenvalues differed from the trace by less than one part in 10^6. Next one can ask whether or not the first eigenvalue of the matrix is a good approximation to the first eigenvalue of the Orr–Sommerfeld equation. Thomas (1953) has calculated c_1, the eigenvalue which corresponds to the least stable mode, for eighteen sets of values of α and R.† In general it was found that for sufficiently large values of N there is agreement to four significant figures between Thomas's values and those obtained by the present method. The only major difference occurs in the value of $\mathrm{Im}\,(c_1)$ for $\alpha = 2{\cdot}4$ and $R = 5000$. Thomas lists the value 0·0170 and we find 0·010661. It appears likely that this is a misprint in Thomas's paper. A further comparison is provided by the eigenfunction. Thomas tabulates the first eigenfunction for $\alpha = 2{\cdot}0$, $R = 20{,}000$. The maximum relative deviation between our results and those of Thomas is about 3 % and occurs very near the wall where the eigenfunction itself is very small.

The effect of truncation, i.e. the number of terms retained in the expansion of ϕ, has been examined in some detail. For fixed values of α and R the size of the matrix (N) was increased until the value of c_1 became insensitive to the precise value of N. At this point it was generally found that the next few eigenvalues

† Note again that the values of α and R given by Thomas are exactly half of those in this paper because of the different length scale. Thomas's values of α and R have been adjusted to the length normalization used in this paper.

$\mathrm{Im}(c_1) \times 10^4$	$\alpha = 2{\cdot}20$	2·16	2·12	2·08	2·04	2·00	1·90	1·80	1·70	1·60	1·50	1·40
						R						
2	10,700	9,500	9,400	9,300	9,700	10,000	10,600	12,100	14,400	17,300	21,900	28,700
	28,700	35,300	43,000	51,500								
0	—	13,200	12,100	11,600	11,500	11,600	12,500	14,000	16,300	19,700	25,000	33,000
		26,000	34,000	41,300	50,000	60,000						
−2	—	—	—	16,200	15,000	14,500	14,900	16,400	18,900	23,000	29,100	38,000
				29,100	38,100	47,800						
−4	—	—	—	—	—	23,000	19,000	20,000	22,500	27,300	34,300	45,200
						30,000	59,000					
−6	—	—	—	—	—	—	—	26,500	28,400	33,900	42,400	57,000
								71,000				

TABLE 1. Constant amplification curves. Note that R is a double-valued function of α and $\mathrm{Im}(c_1)$

had also become virtually independent of N. For example, for

$$\alpha = 2{\cdot}0, \quad R = 20{,}000,$$

the eigenvalues were calculated for $N = 20$, 30, 40 and 50. Examination of the results showed that as N was increased there was a rapid convergence of the value of c_j to a limit. Taking $N = 30$ yielded at least the first ten eigenvalues with an accuracy of about 1 %. For $N = 40$ the accuracy was about 0·1 %. Similar calculations were also carried out for $\alpha = 2{\cdot}2$, $R = 70{,}000$. Even for this large value of αR it was found that $N = 30$ gave the first eigenvalue with an error of about 15 % in the imaginary part of c_1 and eigenvalues two to four with an error of about 1 %. For $N = 40$ the first eleven eigenvalues were found with an accuracy of about 1 %.

3.2. *Eigenvalue of the least stable mode*

The eigenvalues for a symmetric disturbance streamfunction have been computed as a function of Reynolds number for a fixed value of α. The values of α chosen ranged from 1·0 to 2·4 and the Reynolds number varied from 3200 to 52,000. A table (table A) of the value of the first eigenvalue, c_1, for all of these cases has been deposited with the editor. The imaginary part of c_1 is plotted versus R for fixed α in figure 1 and the real part of c_1 is plotted versus R for fixed α in figure 2. From these figures it is apparent that $\mathrm{Im}\,(c_1)$ is a complicated function of α and R but that $\mathrm{Re}\,(c_1)$ is, at least over the range of α and R considered, a monotonically decreasing function of R for fixed α and a monotonically increasing function of α for fixed R.

From figure 1, constant amplification rate curves, i.e. the loci of values of α and R such that $\mathrm{Im}\,(c_1) =$ constant, can be obtained. This has been done and the results are listed in tables 1 and 2. In figure 3 the curves of constant amplification rate and the curves of constant wave speed are plotted in the (α, R)-plane. The neutral stability curve is indicated by $\mathrm{Im}\,(c_1) = 0$. Also shown on figure 3 are points on the neutral curve computed by Stuart (1954) and Lock (1956). The neutral curve $(\cdot\text{—}\cdot)$ obtained by Shen (1954) is also shown. (Shen's curve is reproduced in Lin 1955.) The points given by Stuart and Lock, as well as Shen's curve, were obtained using variants of the asymptotic method. It is clear that asymptotic methods give the same results as the expansion method used here on the lower branch of the stability curve. This is just the region, large R and small α, for which the asymptotic method is expected to be best. On the upper branch and near the critical point there is substantial disagreement between the various asymptotic methods and the expansion technique although Lock's results appear to be the most accurate of those obtained with asymptotic methods. Shen obtained a critical Reynolds number $R_c = 10{,}600$ and $\alpha_c = 2{\cdot}15$; Thomas found $R_c = 11{,}560$, $\alpha_c = 2{\cdot}052$; and the present method gives

$$R_c = 11{,}500, \quad \alpha_c = 2{\cdot}05.$$

The eigenvalues for the antisymmetric disturbance streamfunction have also been calculated for values of α from 1·6 to 2·4 and values of the Reynolds number from 5000 to 52,000. The value of the first eigenvalue for each of these

cases is listed in table B which has been deposited with the editor. The imaginary part of c is plotted in figure 4 versus R for fixed α. It is apparent from figure 4 that the imaginary part of c is proportional to $R^{-\frac{1}{2}}$, at least over the range of R

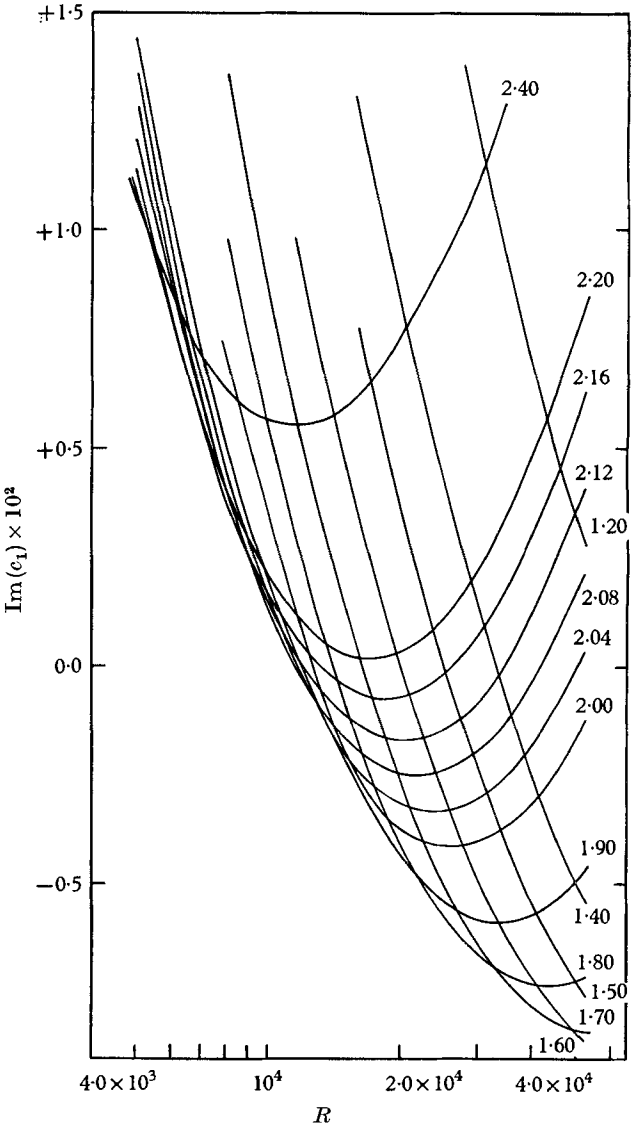

FIGURE 1. Imaginary part of the first eigenvalue (Im(c_1)) of the symmetric disturbance streamfunction versus R for various values of α. The numbers next to the curves are the values of α.

considered here. The eigenvalue whose imaginary part is plotted in figure 4 is c_4 since for these values of α and R the imaginary part of c_2 lies above the imaginary part of c_4. Based on this study it can be concluded that disturbances with an antisymmetric streamfunction are stable for $R \lesssim 50{,}000$ and it is probable that they are stable for all R.

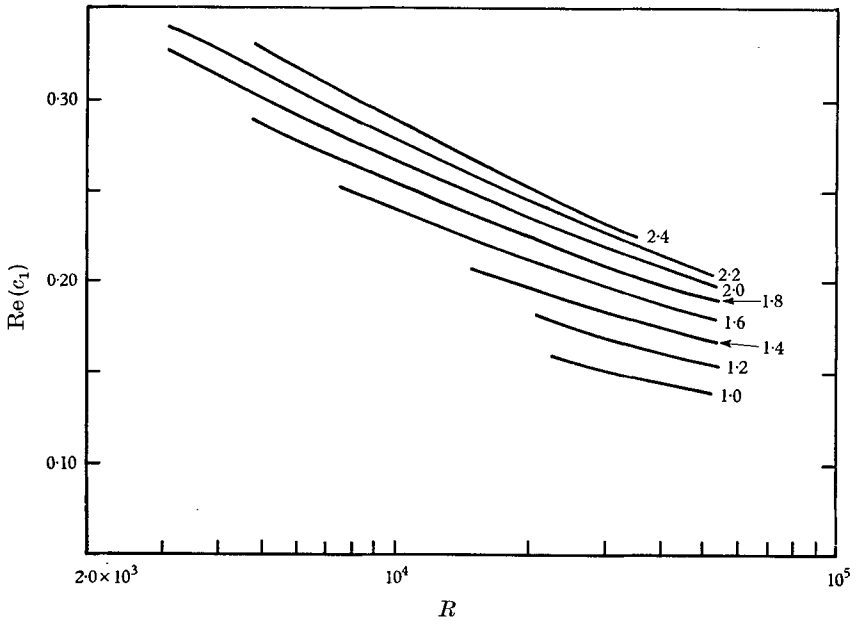

FIGURE 2. Real part of the first eigenvalue ($\mathrm{Re}(c_1)$) of the symmetric disturbance stream-function versus R for various values of α. The numbers next to the curves are the values of α.

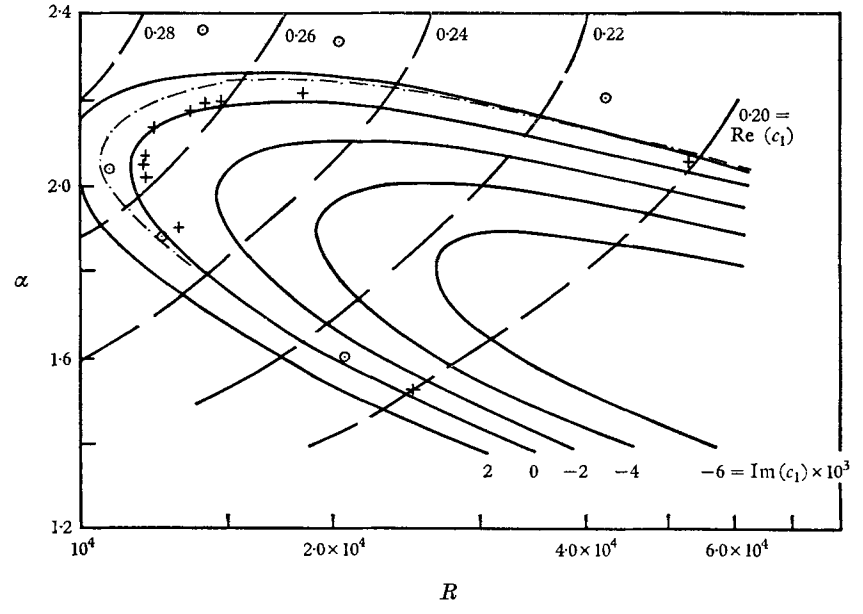

FIGURE 3. Curves of constant amplification, $\mathrm{Im}(c_1)$ = constant (solid line). Curves of constant phase velocity, $\mathrm{Re}(c_1)$ = constant (dashed line). These curves have been obtained by the expansion technique. Results of asymptotic method for neutral stability curve: dash-dot line, Shen (1954); ⊙, Stuart (1954); +, Lock (1956).

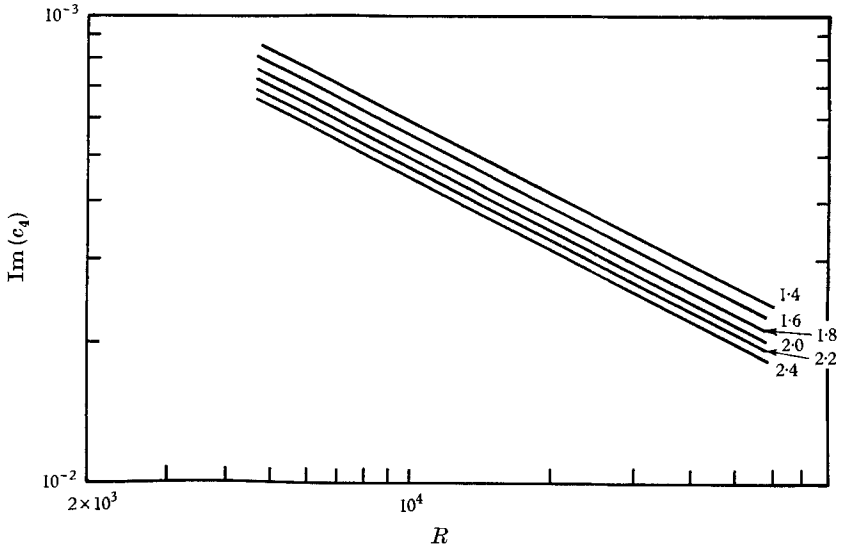

FIGURE 4. Imaginary part of the least stable eigenvalue ($\mathrm{Im}(c_4)$) of the antisymmetric disturbance streamfunction versus R for various values of α. The numbers next to the curves are the values of α.

$\mathrm{Re}(c_1)$ =	0·30	0·28	0·26	0·24	0·22	0·20	0·18
				R			
α							
2·40	8,200	11,860	17,440	26,000	40,000	—	—
2·20	6,640	9,900	14,800	23,000	36,000	60,000	—
2.00	5,120	7,800	12,000	18,500	30.000	50,200	—
1·90	4,360	6,740	10,400	16,500	26,800	45,600	—
1·80	3,640	5,680	8,960	14,200	23,200	39,500	—
1·70	—	—	7,460	12,160	19,800	33,600	60,000
1·60	—	—	—	10,100	16,800	28,400	51,600
1·50	—	—	—	—	14,000	23,800	42,400
1·40	—	—	—	—	—	19,100	37,800
1·20	—	—	—	—	—	—	21,400

TABLE 2. Constant wave-speed curves

3.3. *The higher eigenvalues*

As was mentioned above, if N is taken sufficiently large then we obtain a number of the higher eigenvalues. To our knowledge only Grohne (1954) has calculated any of the higher eigenvalues for plane Poiseuille flow and the disagreement between his results for plain Couette flow and those of Gallagher & Mercer (1964) casts doubt on the accuracy of Grohne's results for plane Poiseuille flow.

Grohne calculated the first four eigenvalues for (in our notation) $\alpha = 1{\cdot}74$ and R between about 2×10^3 and 10^7. We have calculated the first four eigenvalues for $\alpha = 1{\cdot}74$ and Reynolds numbers up to about 50,000. In figure 5 we show our results and Grohne's. It is evident that there is considerable disagreement.

There is agreement in the general trend of the imaginary part of the eigenvalues but the magnitudes do not agree well. As for the real part, there is complete disagreement on the results for eigenvalues three and four. It would appear, in the light of our results and those of Gallagher & Mercer, that Grohne's results are not reliable.

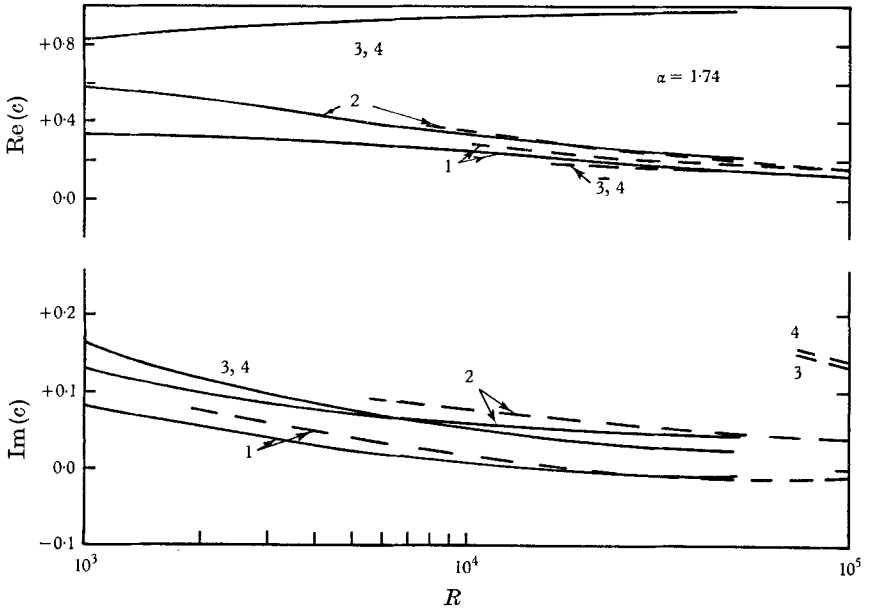

FIGURE 5. Real and imaginary parts of the first four eigenvalues versus R for $\alpha = 1{\cdot}74$. Grohne's results, dashed curves; expansion technique, solid curves.

In order to gain further insight into the behaviour of the various modes, the spectrum of eigenvalues has been examined in some detail for a single fixed wave-number ($\alpha = 2{\cdot}0$) as the Reynolds number was varied from 1 to 50,000. For $R \lesssim 100$ the behaviour of the eigenvalues is particularly simple. The real parts of the c_n are independent of R and, with two exceptions, tend to group around a value of $\frac{2}{3}$, which is the average velocity in the channel. The imaginary parts of the c_n are proportional to R^{-1}. It is convenient to order the eigenvalues with respect to the size of the imaginary part of c_n at low Reynolds number. It is then found that c_1, c_3, c_5, c_7, ... are the eigenvalues of the symmmetric stream-functions and c_2, c_4, c_6, c_8, ... are the eigenvalues of the antisymmetric stream-functions. The real and imaginary parts of c_1 to c_8 are plotted in figures 6 and 7.

Several points should be noted from these figures. Only Im (c_1) becomes negative and hence there is only one unstable mode. This has been found to be true for all values of α for which the eigenvalues have been calculated and this indicates that there is probably never more than one unstable mode. The order of the eigenvalues is not maintained for $R \gtrsim 800$. The eigenvalues shown here can be generally divided into two groups for $R > 1000$. There is a group of fast modes for which Re (c_n) > 0·9 and is apparently asymptotic to 1·0. This group includes, of those shown in figures 6 and 7, modes 3, 4, 5, 6, and 8. The Im (c_n) for these

modes has very similar behaviour and in fact eigenvalues 3 and 4 coalesce as do 5 and 6. Although it is not shown, there is another eigenvalue whose imaginary

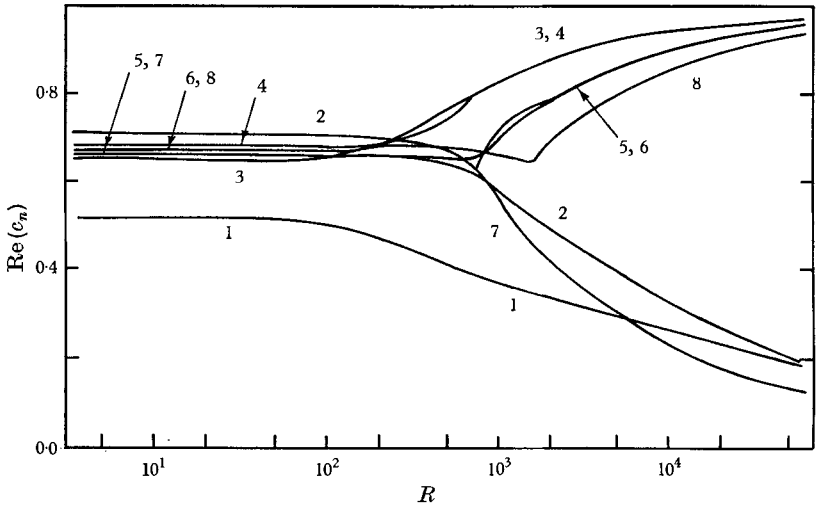

FIGURE 6. Real parts of the first eight eigenvalues versus R for $\alpha = 2{\cdot}0$. Note that ordering of the eigenvalues is by the magnitude of the imaginary part of the eigenvalue at low R.

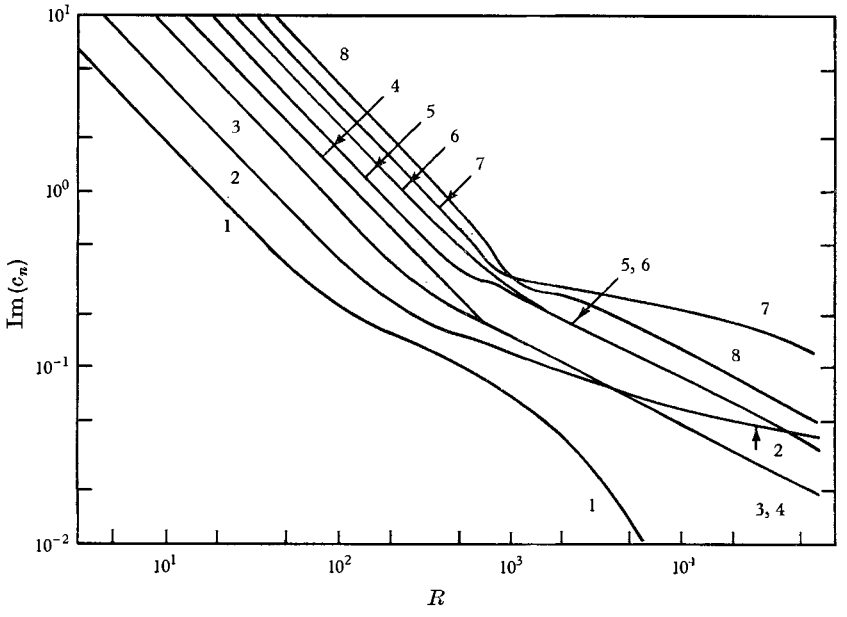

FIGURE 7. Imaginary parts of the first eight eigenvalues versus R for $\alpha = 2{\cdot}0$. Note that the crossings do not represent degeneracies since the real parts of the eigenvalues are not equal at the points where the imaginary parts are, and vice versa.

part coalesces with c_8. There is also a group of slow modes for which Re (c_n) is a decreasing function of R. These include modes 1, 2 and 7. It should be noted that Im (c_2) and Im (c_7) have similar behaviour which is different from that of the

'fast modes.' Finally, it should be noted that, although some of the eigenvalues coalesce, that is, become degenerate at high R, the crossings in figures 6 and 7 do not represent degeneracies since the real parts are different where the imaginary parts cross and vice versa.

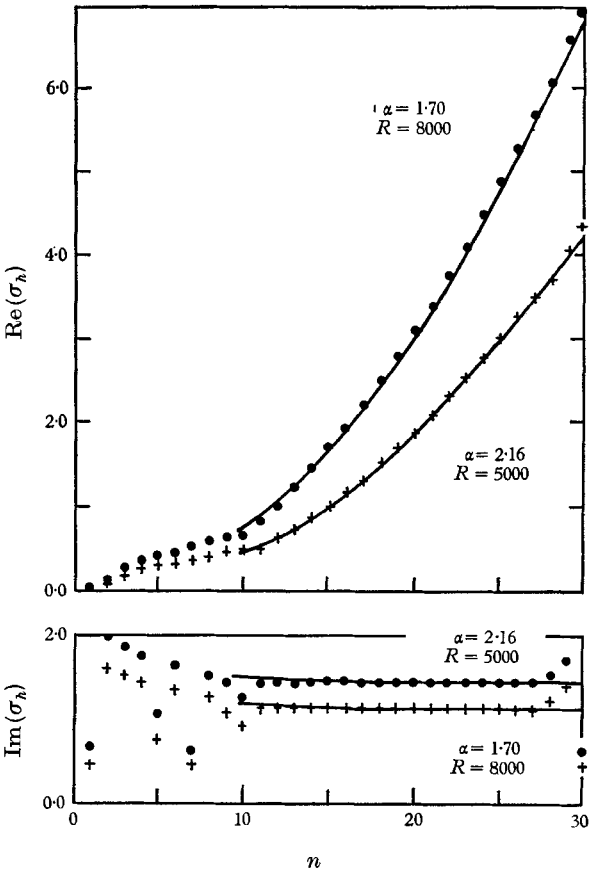

FIGURE 8. Comparison of the asymptotic formula for the eigenvalues of a symmetric disturbance streamfunction with the numerical values obtained from the matrix. ●, $\alpha = 2{\cdot}16$, $R = 5000$; +, $\alpha = 1{\cdot}70$, $R = 8000$.

Although the numerical calculations yield only the first N eigenvalues it is possible to obtain the entire spectrum for any particular value of α and R. As was discussed in §2.3, ϕ is approximated by the first N terms in the series expansion. This approximation is only valid if the higher modes are decoupled from all other modes. If the higher modes are decoupled, then it is possible to derive an approximate expression for the higher eigenvalues. If mode n is decoupled then (equation (33)) only the diagonal matrix element F_{nn} is retained in the equation for a_n. Therefore, the amplitude function $a_n(t)$ is the solution of

$$\frac{da_n}{dt} = F_{nn}\, a_n. \tag{57}$$

Since F_{nn} is a constant, the nth eigenvalue σ_n equals F_{nn}. This can be true only

for large n and so $\beta_n \approx \gamma_n \approx \lambda_n$. Evaluating the matrix elements and substituting λ_n for β_n and γ_n yields

$$\sigma_{2n-1} \approx -(\lambda_n^2/R) + i\alpha(\tfrac{2}{3} + 2/\lambda_n) \tag{58}$$

for disturbances with a symmetric streamfunction. The analogous expression for the disturbances with an antisymmetric streamfunction is

$$\sigma_{2n} \approx -(\mu_n^2/R) + i\alpha(\tfrac{2}{3} + 2/\mu_n). \tag{59}$$

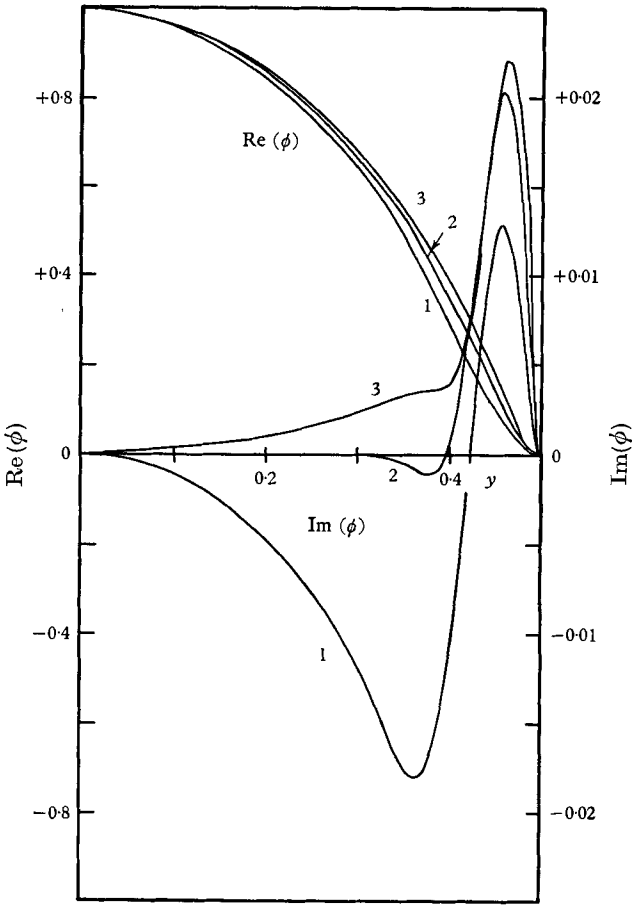

FIGURE 9. Real and imaginary parts of the streamfunction of a symmetric disturbance. For all, $\alpha = 2{\cdot}0$.

	R	C
1	5,000	$0{\cdot}301135 + i0{\cdot}014182$
2	11,600	$0{\cdot}261294 + i0{\cdot}000044$
3	20,000	$0{\cdot}237413 - i0{\cdot}003681$

For a given α and R, if N is large enough, the upper eigenvalues of the matrix will overlap the region where the asymptotic expression for the eigenvalue is valid. Therefore the first N eigenvalues, σ_1 to σ_n, are the eigenvalues of the matrix and σ_n for $n > N$ is given by the asymptotic formula. In figure 8 the first 30 eigenvalues, for a symmetric streamfunction, obtained from the matrix

have been plotted for two different cases, $\alpha = 2{\cdot}16$, $R = 5000$, and $\alpha = 1{\cdot}70$, $R = 8000$. Previous calculation had shown that for these values of α and R only about 20 terms are needed in the approximate expansion of ϕ. The last 10 eigenvalues ought then to agree with the asymptotic formula. The real and imaginary parts of σ_n as given by the asymptotic formula, equation (58), are also plotted in figure 8. It is clear that, except for a truncation error on the last two points, the agreement is excellent. This also indicates that for $n > N$ the nth eigenfunction is approximately $C_n(y)$.

3.4. *The eigenfunctions*

Once the eigenvalues are known it is possible to obtain the eigenfunctions from a set of N linear equations with zero secular determinant. These equations can be solved to obtain the ratio of each coefficient to the first. The set of values $[a_n/a_1]$ or $[b_n/b_1]$ determines ϕ to within a multiplicative constant.

The first eigenfunction has been calculated for a number of values of α and R, corresponding to both stable and unstable conditions. Figure 9 shows the real and imaginary parts of ϕ for $\alpha = 2{\cdot}0$ and $R = 5000$ (stable), 11,600 (on the neutral curve), and 20,000 (unstable). The normalization adopted is $\phi(0) = 1$. The most striking feature is the relative smallness of $\mathrm{Im}\,(\phi)$. In fact

$$|\mathrm{Im}\,(\phi)| \leqslant 0{\cdot}025$$

in all cases. Other features are that $\mathrm{Re}\,(\phi)$ is nearly independent of α and R and that $\mathrm{Im}\,(\phi)$ peaks up at $y \approx 0{\cdot}45$. The major difference between stable and unstable conditions would appear to be the negative peak in $\mathrm{Im}\,(\phi)$ for stable conditions. We have calculated the streamfunction for a number of other conditions and we always find the same general behaviour shown in figure 9.

4. Results for modulated plane Poiseuille flow

We next consider the stability of the time-dependent plane Poiseuille flow resulting from modulating the pressure gradient. Specifically we choose the pressure gradient to be

$$\frac{\partial p}{\partial x} = \left(\frac{-8}{R}\right)[1 - \Lambda\cos(\omega t)]. \tag{60}$$

Here Λ is the dimensionless amplitude of the pressure oscillation and ω is the dimensionless frequency of oscillation. The velocity field resulting from applying this pressure gradient between parallel plates is

$$\begin{aligned} U = {} & 1 - 4y^2 - 4\Lambda k^{-2}\sin(\omega t) \\ & + 4\Lambda k^{-2}(x_1^2 + x_2^2)^{-1}\{[x_1\cos(ky)\cosh(ky) + x_2\sin(ky)\sinh(ky)]\sin(\omega t) \\ & + [x_2\cos(ky)\cosh(ky) - x_1\sin(ky)\sinh(ky)]\cos(\omega t)\}, \end{aligned} \tag{61}$$

where

$$k^2 = \tfrac{1}{2}\omega R = \pi l^2/\nu\tau, \tag{62}$$

$$x_1 = \cos(\tfrac{1}{2}k)\cosh(\tfrac{1}{2}k), \tag{63}$$

and

$$x_2 = \sin(\tfrac{1}{2}k)\sinh(\tfrac{1}{2}k). \tag{64}$$

The velocity field consists of three parts, a steady parabolic profile due to the steady part of the pressure gradient, a constant profile which is out of phase with the oscillating part of the pressure gradient, and a shear wave (the term in the curly brackets) which matches the uniform oscillating flow to the zero velocity boundary condition. The characteristic thickness, δ, of the shear wave is

$$\delta = l/k \tag{65}$$

where l is the width of the channel. It is clear that only if the driving frequency is very low, or R is small, will δ be comparable to l.

It is clear from equation (61) that the velocity profile is symmetric about $y = 0$ and so the cross-coupling matrices J and K are again identically zero. Thus even for the time-dependent flow the symmetric and antisymmetric disturbances are decoupled. Only disturbances with a symmetric streamfunction will be considered since these are the only ones which led to instabilities in the steady flow. Therefore, the coefficients in the expansion of ϕ are the solution of

$$\frac{d\mathbf{A}}{dt} = F(t)\,\mathbf{A}, \tag{66}$$

with F given by equation (34).

Equation (66) is equivalent to N first-order differential equations. This set of N equations was numerically integrated N times from $t = 0$ to $t = \tau$. The initial conditions for the first integration are $a_1(0) = 1{\cdot}0$, $a_j(0) = 0$ for $j = 2, 3, \ldots, N$; for the second integration $a_1(0) = 0$, $a_2(0) = 1{\cdot}0$, $a_j(0) = 0$ for $j = 3, 4, \ldots, N$; etc. The numerical integration was carried out using Ralston's fourth-order Runge–Kutta method (Ralston 1962). This gave $W(\tau)$, see equation (50), and the eigenvalues of W were calculated using the same routine which was used in the case of steady flow.

4.1. *Accuracy of the calculations*

The technique was tested by setting $\Lambda = 0$. Then the F matrix is independent of time and the eigenvalues of Q should be identical with the eigenvalues of F. The disturbance wave-number was taken to be $\alpha = 2{\cdot}04$ and the Reynolds number $R = 11{,}750$. These values were chosen because they corresponded to a point very nearly on the stability boundary and it was believed that this would provide a severe test of the method since near the stability boundary $|\mathrm{Im}\,(c_1)|$ is very small and this implies that $|\epsilon_1|$ is very close to unity. Therefore, a small error in ϵ_1 would result in a large error in $\mathrm{Im}\,(c_1)$. The largest error occurred, as was expected, in the imaginary part of c_1. From F it was found that

$$\mathrm{Im}\,(c_1) = -2{\cdot}0 \times 10^{-5}$$

and from Q it was found that $\mathrm{Im}\,(c_1) = -2{\cdot}1 \times 10^{-5}$. For all other eigenvalues the differences were less than or about equal to 0·1 %.

4.2. *Effect of varying the frequency*

It can easily be shown that, if α, R and Λ are held fixed and ω is varied, the amplitude of the velocity oscillations in the base flow will vary with ω. In this case the

amplitude of the pressure oscillation is constant but the amplitude of the velocity oscillation varies. It is also possible, by varying Λ as well as ω, to keep the amplitude of the velocity oscillation constant while the amplitude of the pressure oscillation varies.

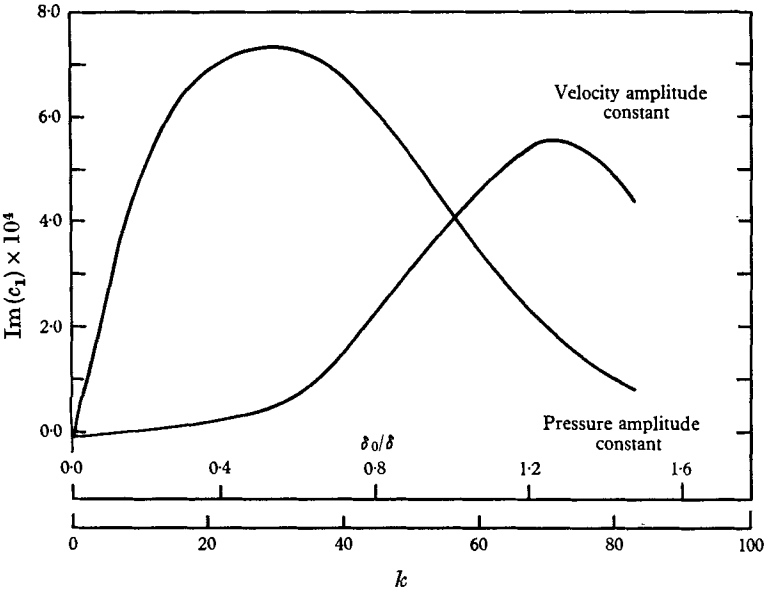

FIGURE 10. The imaginary part of the eigenvalue of the least stable mode (Im (c_1)) versus the frequency parameter k. The wave-number is $\alpha = 2{\cdot}04$ and the Reynolds number $R = 11{,}750$.

A series of calculations was carried out in which the disturbance wave-number α and the Reynolds number R were held constant while the amplitude of the oscillating part of the pressure gradient, as well as the frequency, was varied so that the amplitude of the oscillating part of the velocity in the base flow was held constant while the frequency of oscillation varied. The numerical values chosen were $\alpha = 2{\cdot}04$ and $R = 11{,}750$. This corresponds to a point just within the steady stability boundary; the wave number is equal to the critical wave-number and the Reynolds number is only slightly larger than the critical Reynolds number. It is expected that the frequencies of interest are those which are comparable to the frequency of the unstable mode. This frequency is given by

$$\omega_1 = \alpha \mathrm{Re}\,(c_1) \tag{67}$$

and for these conditions $\omega_1 \approx 0{\cdot}55$. Calculations have been run for a range of frequencies between about $\frac{1}{8}\omega_1$ and $2\omega_1$. As ω was varied, k of course varied, and Λ was adjusted so that the amplitude of the velocity oscillation was kept constant. The results are shown in figure 10, where Im (c_1) is plotted as a function of k. The effect of the modulation is to increase Im (c_1) and hence to stabilize the flow.

Lin (1955) has shown that the disturbance very near the wall has the form of a shear wave with an e-folding length,

$$\delta_0/l \approx (2/\omega_1 R)^{\frac{1}{2}}. \tag{68}$$

The ratio of the characteristic lengths of the disturbance shear wave and the driving shear wave due to the oscillation is

$$\delta_0/\delta = k^{-1}(2/\omega_1 R)^{\frac{1}{2}} = (\omega/\omega_1)^{\frac{1}{2}}. \tag{69}$$

A scale of δ_0/δ is also shown on figure 10. It can be seen that the major stabilization occurs when δ is comparable to δ_0 and this suggests that the shear wave due to the modulation interferes with the disturbance shear wave and decreases the rate of energy transfer from the base flow to the disturbance, thus stabilizing the flow.

These results for periodically modulated flows are very precise. However, in an attempt to gain further understanding of the mechanism by which the flow is stabilized, we have examined the energy equation for the disturbance. The energy equation is of exactly the same form for a time-dependent base flow as for a steady base flow. Thus, just as in the steady case (see Lin 1955, p. 59), the flow can become unstable only if the product of the Reynolds stress and the gradient of the base flow, when integrated between the boundaries, is positive and large enough to outweigh the dissipation due to viscosity. Assuming that Λ is small, we have considered a perturbation expansion in Λ. We examined, following Lin, the form of the vorticity very near the wall. The zero-order term (in Λ) in the expansion of the vorticity satisfies a homogeneous diffusion equation but the first-order term is determined by an inhomogeneous diffusion equation. The forcing term contains the product of zeroth-order terms in the disturbance velocity and its derivatives with first-order terms in the base flow velocity and its derivatives. This provides the coupling of the modulated component of the base flow with the disturbance. After calculating the zeroth- and first-order terms in the vorticity the corresponding velocity components were calculated from the continuity equation and the definition of vorticity. Finally, the Reynolds stress near the wall (averaged over a wavelength of the disturbance and a period of the modulation) was calculated.

The Reynolds stress, τ, is of the form $\tau_0 + \Lambda^2\tau_2$. The term τ_0 is positive and is exactly that found by Lin. If $(\omega/\omega_1)^{\frac{1}{2}} = \delta_0/\delta \gtrsim 1{\cdot}5$ then τ_2 becomes negative and hence tends to stabilize the flow by decreasing the rate of energy transfer from the base flow to the disturbance.

These calculations, which were carried out with the same approximations as used by Lin (1955, p. 62), are discussed here in order to illustrate the mechanism by which the modulation can stabilize the flow. Since they are both lengthy and approximate, we will not reproduce them here.

If the amplitude of the pressure oscillation Λ is kept constant while the frequency is varied then the amplitude of the velocity oscillation will vary with frequency. A number of calculations of this sort have also been carried out and these results are also shown in figure 10. Again the oscillation stabilizes the flow.

In addition to varying the frequency at constant amplitude, the amplitude

can be varied at constant frequency. The results of a number of these calculations are shown in figure 11. Here $\alpha = 2{\cdot}04$ and $k = 56{\cdot}13$. It is seen that, for this range of amplitudes, increasing Λ will monotonically increase $\mathrm{Im}\,(c_1)$ and so stabilize the flow.

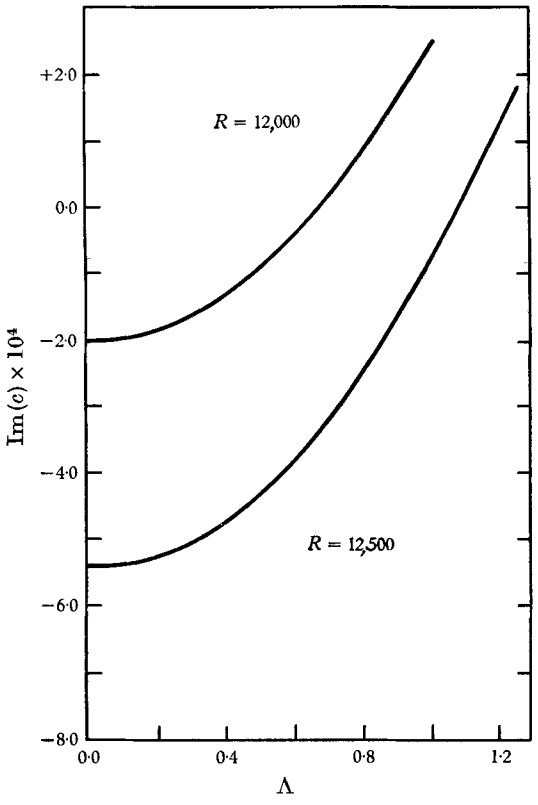

FIGURE 11. The imaginary part of the eigenvalue of the least stable mode ($\mathrm{Im}\,(c_1)$) versus Λ, the amplitude of the pressure modulation. The wave-number is $\alpha = 2{\cdot}04$ and the frequency parameter is $k = 56{\cdot}13$.

For larger modulation amplitudes the effects are somewhat more complex. We have carried out detailed calculations for $\alpha = 2{\cdot}04$, $R = 11{,}750$, $k = 56{\cdot}13$, and Λ varying between 0·0 and 100·0. The results are plotted in figure 12. We find that initially as Λ is increased from zero only the lowest eigenvalue is substantially changed. The $\mathrm{Im}\,(c_n)$ $(n \geqslant 2)$ are changed less than about 5 % for Λ in the range from 0·0 to 10·0. On the other hand, in this range $\mathrm{Im}\,(c_1)$ increases nearly quadratically with Λ. It turns out, for this particular case, that $\mathrm{Im}\,(c_1)$ becomes equal to $\mathrm{Im}\,(c_2)$ at Λ approximately equal to 10·0 and hence mode 2 becomes the least stable mode. For $\Lambda < 100$, the eigenvalue of mode 2 is virtually unaffected by the pressure modulation. In fact, in this range the $\mathrm{Im}\,(c_2)$ slowly oscillates between 0·0478 and 0·0501. As Λ is increased further the $\mathrm{Im}\,(c_1)$ first increases and then decreases to a relative minimum at $\Lambda \approx 27$. $\mathrm{Im}\,(c_1)$ then increases, with one oscillation, as Λ is increased. For Λ between 20·5 and 34·5, c_1 is the eigenvalue with the smallest real part. For Λ between 34·5 and 82·0, c_2

is the eigenvalue of the least stable mode. Finally, as Λ is increased further the imaginary part of the eigenvalue of one of the higher modes begins to decrease. At $\Lambda \approx 82$ it is equal to $\mathrm{Im}\,(c_2)$ and at $\Lambda \approx 85{\cdot}5$ it becomes negative, indicating that the flow is now unstable. For larger values of Λ the growth rate of this mode

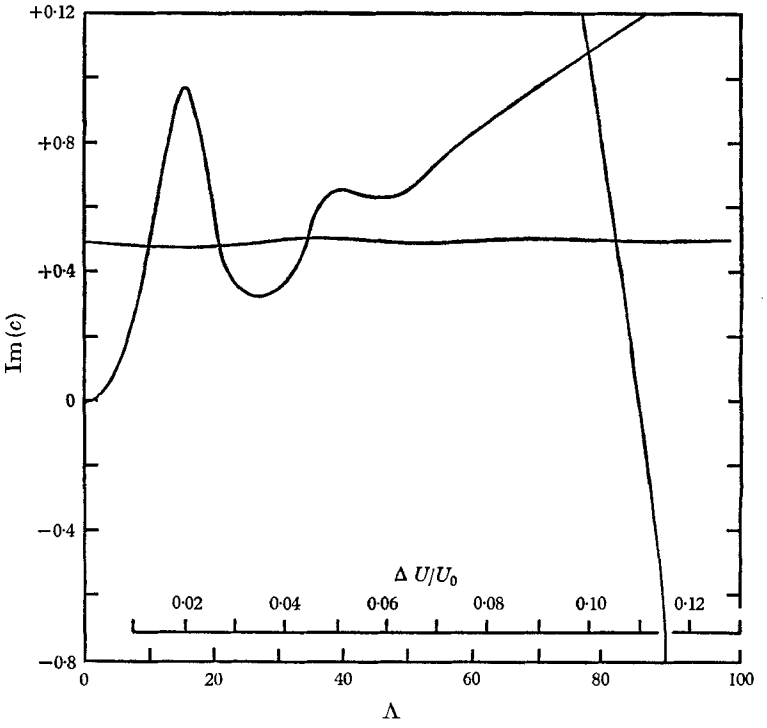

FIGURE 12. Imaginary part of several of the eigenvalues of the least stable modes versus Λ, the amplitude of the pressure modulation. The wave-number is $\alpha = 2{\cdot}04$ and the frequency parameter is $k = 56{\cdot}13$.

is much greater than that of the growing modes in an unmodulated flow. For the steady flow (see figure 3) the $\mathrm{Im}\,(c_1) \gtrsim -0{\cdot}006$ for all Reynolds numbers less than 30,000. For this modulated flow at $R = 11{,}750$, the imaginary part of the eigenvalue is approximately $-0{\cdot}060$ at $\Lambda = 90$.

Although the amplitude of the pressure oscillation is very large, the amplitude of the velocity oscillation is much smaller owing to the high frequency. A scale of $\Delta U/U_0$, where ΔU is the amplitude (in dimensional units) of the velocity oscillation, has been added to figure 12. The transition from very stable to very unstable occurs in a very narrow range, for $\Delta U/U_0$ from about 0·105 to 0·115. At high frequencies, i.e. large k, the viscous shear wave due to the modulation of the pressure gradient is confined to a thin layer near the wall. This layer has a thickness of about $3/k$. In this layer the base flow velocity profile is approximately

$$U \approx 4k^{-1}\{k\zeta - \Lambda k^{-1}[\sin(\omega t) - \exp(-k\zeta)\sin(\omega t + k\zeta)]\}, \tag{70}$$

where ζ is the distance from the wall. If

$$\Lambda k^{-1} \ll 1 \tag{71}$$

then the shear wave hardly distorts the base flow at all. On the other hand, if the amplitude of the pressure oscillation is comparable to k the base flow near the wall is distorted. For

$$\Lambda k^{-1} > 1 \tag{72}$$

there is even a back flow for part of the cycle. It is to be expected that this distortion of the base flow would tend to destabilize the flow.

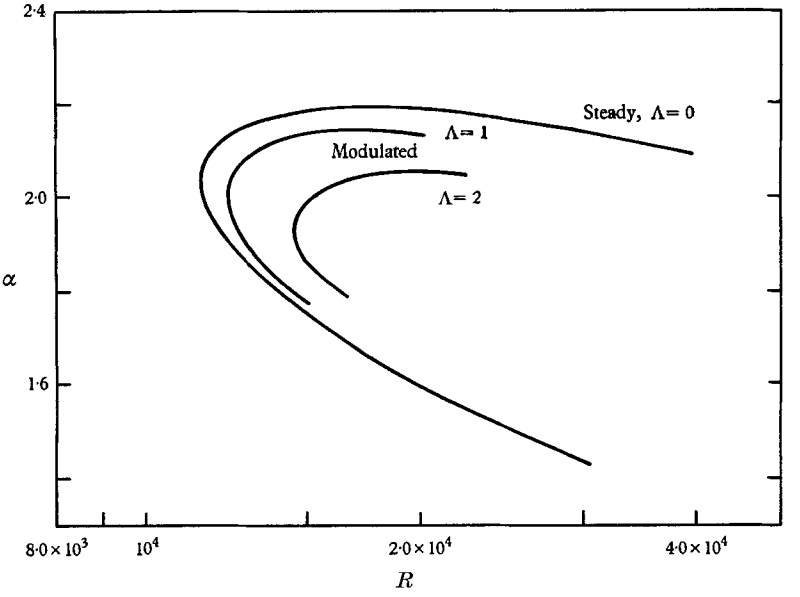

FIGURE 13. Neutral stability curves for steady and modulated plane Poiseuille flow. The frequency parameter is $k = 56{\cdot}13$.

It is clear from the results presented in figures 10, 11 and 12 that modulation can have an appreciable effect on the neutral stability curve. This is shown explicitly in figure 13, which shows the neutral stability curves for $k = 56{\cdot}13$ and $\Lambda = 0$, 1 and 2 ($\Lambda = 1$ corresponds to $\Delta U/U_0 \approx 0{\cdot}0013$). It can be seen that not only is the critical Reynolds number increased by the modulation but the width of the band of unstable wave-numbers is also decreased. From an examination of the results shown in figures 10 and 12 it is apparent that a different choice of modulation frequency and/or amplitude would yield a different stability curve. However, all of these calculations indicate that, provided that the amplitude of the oscillation is not too large, this stability curve would lie inside the steady stability curve. The increase in the critical Reynolds number and the width of the band of unstable wave-numbers depends upon the frequency and amplitude, but it can be inferred from these calculations that modulation of the pressure gradient stabilizes plane Poiseuille flow as long as the amplitude of the oscillation is small. For larger amplitudes of oscillation, it appears that the flow is destabilized by the modulation, with growth rates as much as an order of magnitude greater than that of the steady flow.

5. Discussion

We have studied steady and modulated plane Poiseuille flow by the technique of expansion in a set of orthogonal functions.

For steady plane Poiseuille flow we have calculated to high accuracy the neutral stability curve and curves of constant amplification (or attenuation), both of which are obtained from the eigenvalue of the least stable disturbance.

We have also studied the other disturbance modes and found, for a number of values of the Reynolds number R and the wave-number α, the entire eigenvalue spectrum. As has been conjectured by a number of authors (Shen 1964 for example), no more than one mode is unstable at a given R and α in the region of the (R, α)-plane that we have investigated. The values obtained by Grohne (1954) for the eigenvalues of the four least stable antisymmetrical disturbances are in poor agreement with our results.

We have recalculated, by our method, all of the results obtained by Thomas (1953) by numerical solution of a set of difference equations. In all cases the agreement is excellent.

It has been shown that modulation of the pressure gradient in plane Poiseuille flow can have an important effect on the stability characteristics of the flow. Although it might have been thought, *a priori*, that an oscillating pressure gradient could set up a resonance and so cause instability, such is apparently not the case for small amplitudes of oscillation.

The disturbance has the form of a shear wave near the wall. The oscillating pressure gradient also sets up a shear wave near the wall. It is apparently the interference between these two waves which stabilizes the flow. If the thickness of the shear wave driven by the oscillating pressure gradient is either much larger or much smaller than the thickness of the disturbance shear wave, then the growth rates of the disturbance are not very much affected. However, if the thickness of the two shear waves is comparable then there is apparently an interference leading to a decrease in the rate of energy exchange between the base flow and the disturbances and thus stabilizing the flow. For moderate increases in the amplitude of oscillation, the flow becomes increasingly stable.

For quite large modulation amplitudes the stability of the flow decreases, i.e. the magnitude of $\mathrm{Im}\,(c_1)$ decreases. This appears to be due to the increasing distortion of the base flow by the oscillations. Regions of high shear are produced near the wall and for large enough amplitudes of oscillation there is even reversed flow for part of the cycle. For a modulation velocity amplitude of about 10 % of the steady velocity, the growth rate was found to be an order of magnitude larger than typical growth rates for an unstable disturbance of the steady flow.

At a fixed frequency of oscillation and amplitude the wave-number and Reynolds number have been varied and a neutral stability curve has been obtained. The neutral stability curve for the modulated flow shows a higher critical Reynolds number and a narrower band of unstable wave-numbers than that for the steady flow. It appears that by picking an appropriate modulation frequency and choosing a large enough (but not too large) modulation amplitude the flow can be made stable at very high Reynolds numbers.

There are no experiments with which the results of these calculations can be directly compared. However, the general features which appeared in the Couette (Donnelly *et al.* 1962; Donnelly 1964) and circular pipe Poiseuille (Gilbrech & Combs 1963) flow experiments can also be discerned in the results of these calculations. Modulation will stabilize the flow, and there is apparently an optimum frequency and amplitude of modulation for a given wave-number and Reynolds number. The only other experiments which we know of are those of Miller & Fejer (1964) and Obremski & Fejer (1967) on transition in an oscillating boundary layer. In these experiments oscillations were introduced into the free stream and the transition Reynolds number in the boundary layer was measured.

While it is true that R_t, the transition Reynolds number (the Reynolds number at which turbulent bursts first appear) and not R_c, the critical Reynolds number (the Reynolds number at which the laminar flow becomes unstable) was measured in the boundary layer experiments, it is expected that R_c would have the same qualitative behaviour as R_t. They did not find any stabilizing effect of the oscillations but found instead that the manner in which transition occurs depended on a 'non-steady Reynolds number'. If this number was less than a critical value, transition appeared to be independent of the oscillations. If the 'non-steady Reynolds number' exceeded the critical value, the transition Reynolds number appeared to be independent of the frequency of modulation and to decrease with increasing amplitude of oscillation.

The technique which we have used in this paper can be easily extended to the case of oscillations in a boundary layer. Such a study would seem to be desirable.

One result of this study has been to demonstrate the utility of the expansion technique for studying the stability of steady as well as time-dependent flows. This has been made possible by the development of large, fast digital computers as well as the discovery of new algorithms (which are both rapidly convergent and stable) for calculating the eigenvalues of matrices.

For a steady flow, if only one eigenvalue is sought and a reasonable estimate of this (complex) eigenvalue is available, this technique is relatively no faster than that of Thomas (1953). Thomas's calculations, which used Lin's results as a starting point, took about 300 hours on the SSEC. Our recalculation of Thomas's results on the 7094 took 20 min. The speed ratio of about 900 to 1 is comparable to the speed ratio of the machines used.

The advantages of the expansion technique for a steady flow problem are that it obtains the higher eigenvalues along with the least stable one and that it does not need an approximate value of the eigenvalue as a starting point. We are not aware of any other method for obtaining accurate growth rates for a modulated flow.

One final point concerns Poiseuille flow in a circular pipe. In general the disturbances are three-dimensional and vary as $e^{in\theta}$, where θ is the azimuthal angle. So far, only the axisymmetric modes (those with $n = 0$) have been studied. It has been shown (see e.g. Pekeris 1948) that these modes are stable. We have adapted the method used in this paper to study these three-dimensional dis-

turbances with arbitrary integer n. We are currently studying the stability of the first five azimuthally varying modes.†

The work reported in this paper was begun while C. E. Grosch was still on the staff of the Stevens Institute of Technology and was supported by the U.S. Office of Naval Research under Contract Nonr-263(36). It has been continued at Hudson Laboratories of Columbia University, where he is now a staff member, and is supported by the U.S. Office of Naval Research under Contract Nonr-266(84). This paper is based, in part, on a thesis submitted by C. E. Grosch to the faculty of Stevens Institute of Technology in partial fulfilment of the requirements for the Ph.D. degree. It is Hudson Laboratories of Columbia University Contribution no. 321. Reproduction in whole or in part is permitted for any purpose of the United States Government.

REFERENCES

CHANDRASEKHAR, S. 1961 *Hydrodynamic and Hydromagnetic Stability.* Oxford: Oxford University Press.

CODDINGTON, E. A. & LEVENSON, N. 1955 *Theory of Ordinary Differential Equations.* New York: McGraw-Hill.

CONRAD, P. W. & CRIMINALE, W. O. 1965*a* The stability of time-dependent laminar flow: parallel flows. *Z. angew. Math. Phys.* **16**, 233.

CONRAD, P. W. & CRIMINALE, W. O. 1965*b* The stability of time-dependent laminar flow: flow with curved streamlines. *Z. angew. Math. Phys.* **16**, 569.

DOLPH, C. L. & LEWIS, D. C. 1958 On the application of infinite systems of ordinary differential equations to perturbations of plane Poiseuille flow. *Q. Appl. Math.* **16**, 97.

DONNELLY, R. J. 1964 Experiments on the stability of viscous flow between rotating cylinders, III. Enhancement of stability by modulation. *Proc. Roy. Soc.* A **281**, 130.

DONNELLY, R. J., REIF, F. & SUHL, H. 1962 Enhancement of hydrodynamic stability by modulation. *Phys. Rev. Lett.* **9**, 363.

GALLAGHER, A. P. & MERCER, A. McD. 1962 On the behaviour of small disturbances in plane Couette flow. *J. Fluid Mech.* **13**, 91.

GALLAGHER, A. P. & MERCER, A. McD. 1964 On the behaviour of small disturbances in plane Couette flow; Part 2, The higher eigenvalues. *J. Fluid Mech.* **18**, 350.

GILBRECH, D. A. & COMBS, G. D. 1963 Critical Reynolds numbers for incompressible pulsating flow in tubes, in *Developments in Theoretical and Applied Mechanics, I.* New York: Plenum Press.

GREENSPAN, H. P. & BENNEY, D. J. 1963 On shear-layer instability, breakdown and transition. *J. Fluid Mech.* **15**, 133.

GROHNE, D. 1954 Über das Spektrum bei Eigenschwingungen ebener Laminarströmungen. *Z. angew. Math. Mech.* **34**, 344. (Translated as On the spectrum of natural oscillations of two-dimensional laminar flows. *Tech. Memor. Nat. Adv. Comm. Aero. Wash.* no. 1417.)

GROSCH, C. E. & SALWEN, H. 1967 Hydrodynamic stability of a modulated shear flow. *Phys. Rev. Lett.* **18**, 946.

HAUPT, O. 1912 Über die Entwicklung einer willkürlichen Funktion nach den Eigenfunktionen des Turbulenzproblems. *Sber. bayer. Akad. Wiss.* **2**, 289.

KELLY, R. E. 1965 The stability of an unsteady Kelvin–Helmholtz flow. *J. Fluid Mech.* **22**, 547.

† *Note added in proof*: In addition to our work (Salwen, H. & Grosch, C. 1968 Stability of Poiseuille flow in a circular pipe. *Bull. Amer. Phys. Soc.* **13**, 814), Lessen *et al.* (Lessen, M., Sadler, S. G., & Liu, T. Y. 1968 Stability of pipe Poiseuille flow. *Phys. Fluids*, **11**, 1404) also treats this problem.

KELLY, R. E. 1967 On the stability of an inviscid shear layer which is periodic in space and time. *J. Fluid Mech.* **27**, 657.

LIN, C. C. 1955 *The Theory of Hydrodynamic Stability*. Cambridge University Press.

LOCK, R. C. 1956 The stability of an electrically conducting fluid between parallel planes under a transverse magnetic field. *Proc. Roy. Soc.* A **233**, 105.

MILLER, J. A. & FEJER, A. A. 1964 Transition phenomena in oscillating boundary-layer flows. *J. Fluid Mech.* **18**, 438.

OBREMSKI, H. J. & FEJER, A. A. 1967 Transition in oscillating boundary layer flows. *J. Fluid Mech.* **29**, 93.

PARLETT, B. N. 1967 The *LU* and *QR* algorithms, in *Mathematical Methods for Digital Computers*, II, ed. A. Ralston and H. S. Wilf. New York: John Wiley.

PEKERIS, C. L. 1948 Stability of the laminar flow through a straight pipe of circular cross-section to infinitesimal disturbances which are symmetrical about the axis of the pipe. *Proc. Natl. Acad. Sci. U.S.* **34**, 285.

RALSTON, A. 1962 Runge–Kutta methods with minimum error bounds. *Math. Comp.* **16**, 431.

REID, W. H. 1965 The stability of parallel flows, in *Basic Developments in Fluid Dynamics*, ed. M. Holt. New York: Academic Press.

SCHENSTED, I. V. 1960 Contributions to the theory of hydrodynamic stability. Ph.D. dissertation, University of Michigan.

SHEN, S. F. 1954 Calculated amplified oscillations in the plane Poiseuille and Blasius flows. *J. Aero. Sci.* **21**, 62.

SHEN, S. F. 1961 Some considerations on the laminar stability of time-dependent basic flows. *J. Aerospace Sci.* **28**, 397.

SHEN, S. F. 1964 Stability of laminar flows. In *Theory of Laminar Flows*, ed. F. K. Morse. Princeton: Princeton University Press.

SOUTHWELL, R. V. & CHITTY, L. 1930 On the problem of hydrodynamic stability. I. Uniform shearing motion in a viscous fluid. *Phil. Trans.* A **229**, 205.

STUART, J. T. 1954 On the stability of viscous flow between parallel planes in the presence of a co-planar magnetic field. *Proc. Roy. Soc.* A **221**, 189.

STUART, J. T. 1963 Hydrodynamic stability. In *Laminar Boundary Layers*, ed. L. Rosenhead. Oxford University Press.

TAYLOR, G. I. 1923 Stability of a viscous liquid contained between two rotating cylinders. *Phil. Trans.* A **223**, 289.

THOMAS, L. H. 1953 The stability of plane Poiseuille flow. *Phys. Rev.* **91**, 780.

WILKINSON, J. H. 1965 *The Algebraic Eigenvalue Problem*. Oxford University Press.